

Tissue & Cell

Characterization of stage-specific tyrosinated α -tubulin immunoperoxidase staining patterns in Sertoli cells of rat seminiferous tubules by light microscopic image analysis

John R. Wenz, Rex A. Hess

Abstract. Microtubules are involved in many structural and functional changes that occur in Sertoli cells during the cycle of the seminiferous epithelium. However, few studies have addressed stage-specific changes in the distribution of microtubules that accompany the process of spermatogenesis. This study provides a stage-by-stage immunohistochemical evaluation of Sertoli cell microtubules in paraffin sections of whole rat testes using an antibody to tyrosinated (α -tubulin). Microtubules that contain tyrosinated tubulin are considered to be less stable and are therefore expected to populate Sertoli cells undergoing dynamic changes during spermatogenesis. A quantitative method was developed to analyze the relative tyrosinated (α -tubulin staining in different stages of the cycle. Immunostaining patterns of the stages were separated into five different groups. Stages VII-VIII had the least amount of tyrosinated α -tubulin, while stages IX-XI contained the greatest amount. The staining patterns were consistent with established structural changes in the seminiferous epithelium, such as the formation of ectoplasmic specializations, the presence of microtubule nucleation sites along the periphery of the apical cytoplasm, and the translocation of elongate spermatids from deep crypts in the Sertoli cell to the tubule lumen. These data should provide improved methods for the evaluation of microtubules in the study of Sertoli cell responses to environmental toxicants and testicular diseases.

Keywords: Testis, Sertoli cell, microtubules, stages, tubulin

Introduction

The rat seminiferous epithelium is a complex assembly of germ cells at varying stages of development, maintained by Sertoli cells that span the seminiferous epithelium from base to lumen. Spermatogenesis in the rat has been divided into 14 distinct stages in the cycle, based upon cellular associa-

tions in the germinal epithelium (Leblond & Clermont, 1952; Hess, 1990; Russell et al., 1990). Recognition of stage characteristics has been instrumental in understanding normal structure and function of the seminiferous epithelium and identifying abnormalities in spermatogenesis. Recently, pathologists have become aware of the importance of recognizing stages in the study of mechanisms of chemically induced testicular toxicity (Creasy, 1997).

The Sertoli cell undergoes remarkable morphologic changes during the progression of germ cells through the stages, which reflect changes not only in structure, but also in function (Parvinen, 1993; Russell, 1993). Microtubules are implicated in several of these structural and functional changes and are one

Department of Veterinary Biosciences, University of Illinois,
2001 S. Lincoln, Ave., Urbana, IL 61802, USA.

Received 10 February 1998

Accepted 17 March 1998

Correspondence to: Dr Rex A. Hess. Tel.: +1217 333 8933; Fax:

elements of the Sertoli cell cytoskeleton (Russell, 1993; Vogl et al., 1993). There is strong evidence that microtubules play a role in the secretion of seminiferous tubule fluid (Allard et al., 1993; Richburg et al., 1994) and in the translocation of germ cells within the seminiferous epithelium (Redenbach and Vogl, 1991; Redenbach et al., 1992; Vogl et al., 1993). Furthermore, numerous studies using microtubule-disrupting agents have shown the significance of microtubules in the structural integrity of the Sertoli cell and in turn the whole seminiferous epithelium (Ireland et al., 1979; Russell et al., 1981; Vogl et al., 1983; Allard et al., 1993; Nakai & Hess, 1994)

Numerous studies using electron microscopy, immunofluorescence and immunohistochemistry have provided important insights into the structure and distribution of microtubules in Sertoli cells (Vogl et al., 1993). However, few studies have addressed stage-specific distributions of microtubules and the changes that accompany the process of spermatogenesis (Amlani & Vogl, 1988; Vogl, 1988). This study provides a stage-by-stage immunohistochemical evaluation of Sertoli cell microtubules in paraffin sections of whole rat testes. A commercially available antibody to tyrosinated (α -tubulin) was used to specifically stain Sertoli cell microtubules. Furthermore, a method for quantitative evaluation of relative tubulin staining was developed using National Institutes of Health (NIH) Image software (public domain image analysis software, Wayne Rasband, NIH). These methods and data should prove useful in research into the normal structure and function of Sertoli cells, as well as research into the mechanisms of microtubule disruption by testicular toxicants and diseases.

Material and methods

General

Male Sprague-Dawley rats (90-100 days old; SASCO, Omaha, NE, USA) were housed 2-3 per cage under normal laboratory conditions (12 h light-12 h dark cycle, $72 \pm 2^\circ\text{F}$, $50 \pm 10\%$ relative humidity) with free access to food and water prior to treatment. Tissues for this study were obtained from control animals used in another study.

Histological methods

The rats were anesthetized with sodium pentobarbital and their testes were fixed by vascular perfusion with Bouin's fixative for 10 min. (Hess & Moore, 1993). After perfusion fixation, testicular cross-sections were cut at approximately 3 mm thickness, immersed in Bouin's solution for another 4 h at room temperature, and processed for paraffin embedding and light microscopy. Serial sections were cut at $6 \mu\text{m}$ and floated onto Fisherbrand, Superfrost/Plus microscope slides. The first section from each block was stained using the periodic acid-Schiff (PAS) reaction and hematoxylin to aid in the identification of stages in the seminiferous tubules.

Immunohistochemistry

Serial sections were immersed in 1% hydrogen peroxide in methanol for 30 min to block endogenous peroxidases, followed by an incubation with 5% normal goat serum for 30 min to prevent non-specific binding. The sections were then incubated overnight at 4°C with the primary antibody, monoclonal antityrosinated α -tubulin, 1:16000 dilution (clone TUB- I A2; Sigma, St Louis, MO, USA). The sections were then incubated with a biotinylated anti-mouse secondary antibody (DAKO, Denmark), at a dilution of 1: 100 for 30 min at room temperature. Antibody localization of antigen was accomplished using a Vectastain Elite ABC immunoperoxidase staining kit (Vector Laboratories, CA, USA). Slides were not counterstained because the counterstain obscured qualitative evaluation of finer immunostaining detail, and the basophilic counterstained nuclei had the same grey value as the immunostaining reaction product, which presented problems with segmentation in image analysis. Sections were processed omitting the primary antibody, as a control for non-specific binding of the secondary antibody.

Qualitative analysis of tubulin immunostaining

Immunostained testis sections were examined by light microscopy. Within a tubule, the stage of spermatogenesis was identified and the stage-specific tyrosinated α -tubulin staining pattern of Sertoli cell microtubules was characterized. Low and high power photomicrographs of the stagespecific tyrosinated α -tubulin staining pattern were taken with black and white film with a green filter on an Olympus Vanox T light microscope. Tubules were then combined into stage groups, based upon similarities in tyrosinated α -tubulin staining patterns, as follows: group 1 (stages III-V); group 2 (stages VI - early VII); group 3 (stages late VII-VIII); group 4 (stages IX-XI); group 5 (stages XII-XIV, 1-11).

Relative quantitation of tubulin immunostaining

Digital images of tyrosinated α -tubulin immunostained, seminiferous tubule cross-sections were collected with NIH Image (public domain image processing and analysis software, Wayne Rasband, NIH) on a Macintosh Quadra 840AV using a Sony 3CCD video camera fitted to an Olympus Vanox T light microscope.

Variation in the deposition of immunoperoxidase reaction product is an inherent problem with quantitation of immunohistochemical staining. Therefore, the following procedures were carried out to reduce variation in stain intensity between testis sections and between tubules within a testis section:

1. A constant light intensity was used for all images collected.
2. All images were collected at x 100 magnification with a focused condenser.
3. Background (non-stained) pixels were standardized. Using the 'Start Capture' command, tubules were

centered and focused on the computer monitor. The freehand region of interest (ROI) selection tool was chosen from the NIH Image Tool Box and the crosshairs were placed in the empty lumen of a tubule or adjacent blood vessel. The grey scale value (GSV) read from the Info window was set at I by adjusting the light level with the iris diaphragm of the microscope.

4. The tubules were outlined using the freehand tool and the Get Tubule macro (See Appendix) was used to save the individual tubules.
5. A total of 10 tubules were collected for each of the five stage groups from three different testis sections and assembled into a Stack in NIH Image.
6. Using the skeletonized tubulin macro (See Appendix), the digitized image was filtered and tubulin staining was segmented from the background staining using the 'Autothreshold' command. The segmented image was then converted from grey scale to binary, such that tubulin staining was represented by black pixels and background by white pixels. Using the 'skeletonize' function, regions of tubulin staining were reduced to single pixel wide lines, which created a tubulin staining profile whose extent and branching pattern represented the stage-specific tubulin staining for that tubule. This procedure was used to reduce differences in relative quantitation values due to variation of staining intensity. Relative quantitation of the tubulin skeleton was expressed as a ratio of the tubulin skeleton pixel area over the total pixel area of the whole tubule image. This value was obtained for each stage group by evaluation of the tubule Stacks.

Mean values, standard deviation and standard error of the mean were calculated for each stage group. Means were compared by ANOVA followed by a multiple range analysis to determine significance between groups ($p < 0.05$).

Results

Stage-specific whole tubule characterization of tyrosinated α -tubulin immunostaining

The characteristic staining pattern for tyrosinated α -tubulin in cross-sections of seminiferous tubules was determined at x 100 magnification in normal rat testes. Linear tubulin immunostaining was present from the base to the tubule lumen, corresponding to Sertoli cell microtubules oriented along the longitudinal axis of the cell. This staining produced a radial pattern of tubulin staining in seminiferous tubule cross-sections which exhibited characteristic differences between the stages of spermatogenesis.

Characteristic staining patterns for the different stages of spermatogenesis are described below and shown in Figs I and 2.

Stage 1. This has an irregular radial pattern consisting of long, narrow 'cable-like' structures from the tubule base

through the body region, which branches out in a 'V' shape and surrounds elongate spermatids near the lumen. The intervening regions are largely devoid of staining except within germ cells along the basal lamina of the tubule, which show pale diffuse staining (Fig. 1).

Stage 11. This has an irregular to regular radial pattern consisting of long, narrow 'cable-like' and wide 'band-like' structures. The branching Y-shaped pattern near the lumen extends deeper into the body region than in Stage 1, coincident with the movement of the elongating spermatids deeper within Sertoli cell crypts. The intervening regions are largely devoid of staining except within germ cells along the basal lamina of the tubule, which show pale diffuse staining (Fig. 1).

Stage 111. Here there is a regular radial pattern consisting of wide 'band-like' structures that start more narrowly at the tubule base but are widest at the lumen. Elongating spermatid cytoplasm extends slightly beyond the tubulin staining further into the tubule lumen. The intervening regions are largely devoid of staining except within germ cells along the basal lamina of the tubule, which show pale diffuse staining (Fig. 1).

Stage IV. This also has a regular radial pattern consisting of wide 'band-like' structures, some with a more narrow base than in stages III or V. which extends from the base to their widest point at the tubule lumen. Elongating spermatid cytoplasm extends slightly beyond the tubulin staining into the tubule lumen. The intervening regions are largely devoid of staining except within germ cells along the basal lamina of the tubule, which show pale diffuse staining (Fig. 1).

Stage V. This has a regular radial pattern consisting of wide 'band-like' structures that start more narrowly at the tubule base and are widest at the lumen. Elongating spermatid cytoplasm extends slightly beyond the tubulin staining into the tubule lumen. The intervening regions are largely devoid of staining except within germ cells along the basal lamina of the tubule, which show pale diffuse staining (Fig. 1).

Stages VI-early VII. These stages have an irregular radial pattern consisting of long, narrow 'cable-like' structures that extend from the tubule base, 'fanning out' to a wide 'band' from mid-epithelium up to the tubule lumen, corresponding to the location of the elongating spermatids. The 'fanned out' wide 'band' results in an irregular ring of tubulin staining near the tubule lumen. The intervening regions are largely devoid of staining except within germ cells along the basal lamina of the tubule, which show pale diffuse staining (Fig. 1).

Late stage VII. This has an irregular radial pattern consisting of long, narrow 'cable-like' structures that extend

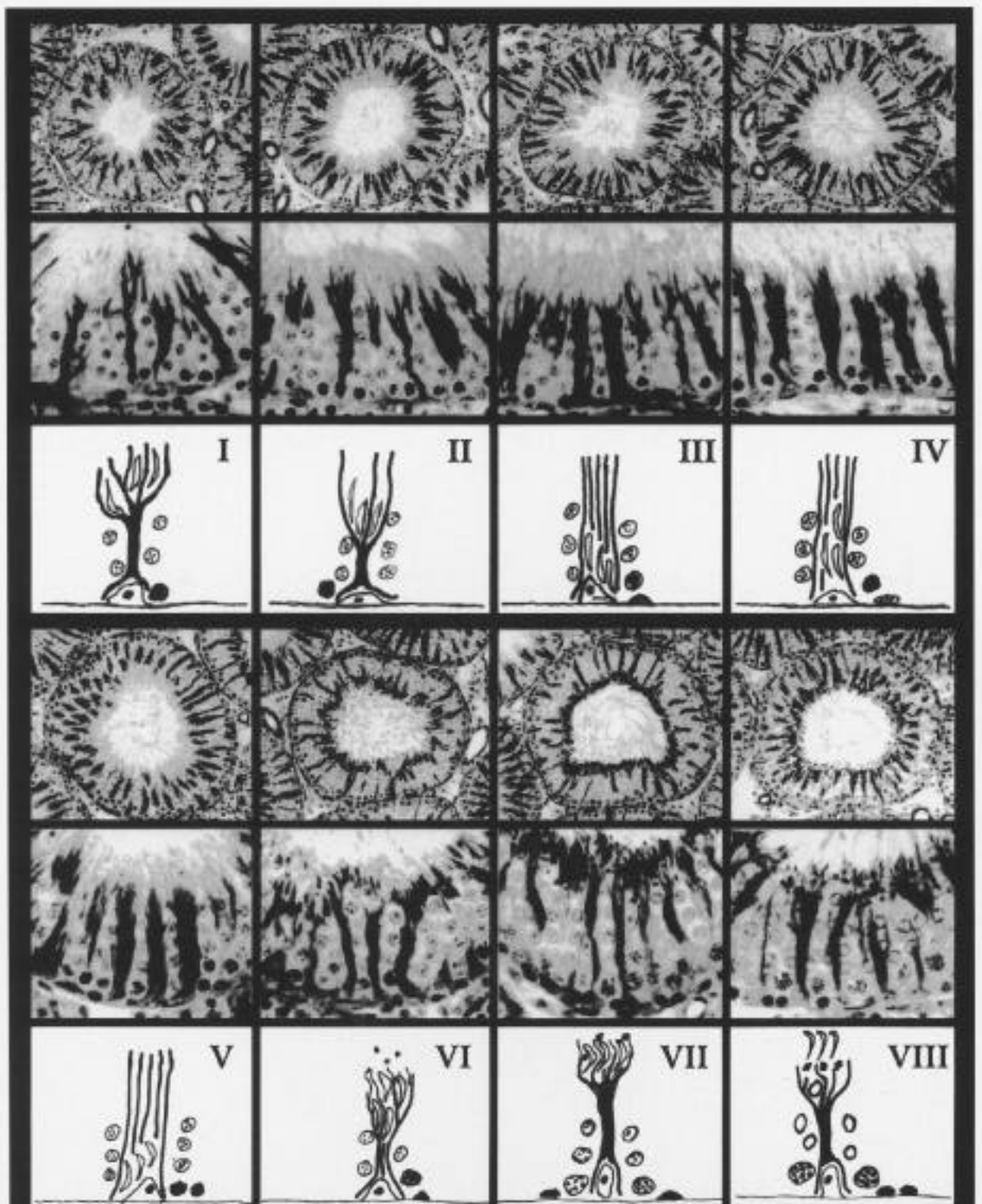


Fig. 1 Immunostaining of tyrosinated α -tubulin in rat seminiferous tubules at stages I-VIII. Rows 1 and 2 are lower and higher magnifications, respectively. Row 3 contains drawings that represent the tubulin pattern. Rows 1 and 4, x 150; rows 2 and 5, x 425.

from the base of the tubule to a regular compact ring of tubulin staining surrounding the elongate spermatid heads lining the tubule lumen. The intervening regions are largely devoid of staining except within germ cells along the basal lamina of the tubule, which show pale diffuse staining (Fig. 1).

Stage VIII. This also has an irregular radial pattern consisting of narrow 'cable-like' structures that are thin at the tubule base. The ring of tubulin staining surrounding the tubule lumen is very thin to absent, but associated with elongate spermatids when present. The intervening regions are largely

from the base of the tubule to a regular compact ring of tubulin

devoid of staining except within germ cells along the

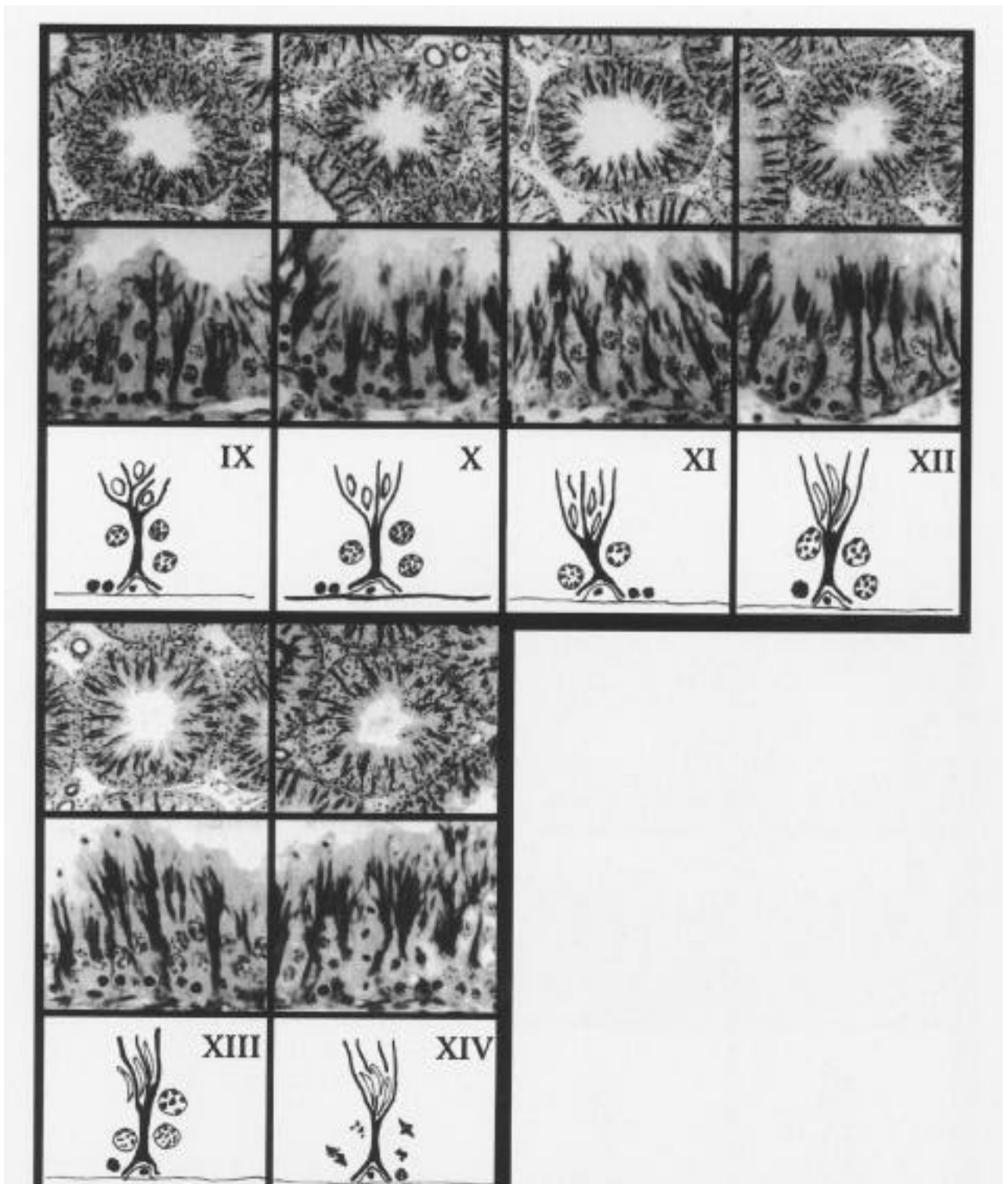


Fig. 2 Immunostaining of tyrosinated α -tubulin in rat seminiferous tubules at stages IX-XIV. Rows 1 and 2 are lower and higher magnifications, respectively. Row 3 contains drawings that represent the tubulin pattern. Rows 1 and 4, x 150; rows 2 and 5, x 425.

basal lamina of the tubule, which show pale diffuse staining (Fig. 1).

Stage IX. This stage has an irregular linear branching staining pattern that surrounds the newly elongating

narrow 'cable-like' structures. The intervening regions, occupied by pachytene spermatocytes, have an even, diffuse staining that makes the whole tubule appear darker than the tubules of previous stages (Fig. 2).

spermatids throughout the apical three-quarters of the **Stages X-XI**. These stages have an irregular, dark,

spermatids throughout the luminal three-quarters of the seminiferous epithelium and extends to the tubule base as short, narrow 'cable-like' structures. The intervening regions, occupied by pachytene spermatocytes, have an evenly, diffuse staining that gives the tubule a darker appearance (Fig. 2).

Stages XII-XIII. These stages have short to long, narrow 'cable-like' staining that is present in the basal one-third of the tubule with wide Y-shaped branching in the luminal two-thirds of the tubule surrounding the elongating spermatids. The elongating spermatid cytoplasm extends well beyond the tubulin staining, into the tubule lumen. Evenly diffuse tubulin staining is present in the intervening regions, giving the tubule a darker overall appearance (Fig. 2).

Stage XIV. This has an irregular radial pattern consisting of short and long, narrow 'cable-like' structures from the tubule base into the body region, branching out in a 'v' shaped pattern and surrounding the elongate spermatids near the lumen. The intervening regions are largely devoid of staining except within germ cells along the basal lamina of the tubule, which show pale diffuse staining and staining of meiotic spindles within cells in diakinesis (Fig. 2).

It was apparent from the observations of individual stages that tubules could be placed into five groups based upon a common tyrosinated α -tubulin staining pattern (Fig. 3). These groups are described below.

Group 1 (stages III-V). This group is characterized by a regular radial pattern of wide 'band-like' structures that start more narrowly at the tubule base but expand to their widest reach near the lumen. The intervening regions are largely devoid of staining except within germ cells along the basal lamina of the tubule which show pale diffuse staining (Fig. 3).

Group 2 (stages VI-early VII). This is characterized by an irregular, radial pattern of long, narrow 'cable-like' structures and an irregular, wide ring of tubulin staining lining the tubule lumen. The intervening regions are largely devoid of staining except within germ cells along the basal lamina of the tubule which show pale diffuse staining (Fig. 3).

Group 3 (stages late VII-VIII). This is characterized by an irregular radial pattern of long, narrow 'cable-like' structures that are thin at the tubule base. A regular, narrow ring of tubulin staining, around the elongate spermatids, lines the tubule lumen. The intervening regions are largely devoid of staining except within germ cells along the basal lamina of the tubule which show pale diffuse staining (Fig. 3).

Group 4 (IX-XI). This is characterized by numerous, thick, dark staining branches in the luminal two-thirds of the tubule surrounding the newly elongating spermatids. An evenly diffuse staining pattern is observed within pachytene

spermatocytes, which produces an overall darker staining appearance for the tubules (Fig. 3).

Group 5 (XII-XIV, 1-11). This is characterized by 'v'-shaped, luminal branches that are thinner, lighter and less extensive than those of group 4. Diffuse tubulin staining is present within pachytene spermatocytes. The overall tubulin staining pattern is lighter than in group 4 and the branching pattern is finer throughout. The intervening regions of stage XIV tubules are largely devoid of tubulin staining with meiotic spindles stained in cells during diakinesis (Fig. 3).

Relative quantitation of tubulin immunostaining using image analysis

Using immunostained testis cross-sections with no counterstain, the skeletonized tubulin staining patterns of individual seminiferous tubule images were analyzed by group. A representative tubule and corresponding skeletonized image from each group is shown in Fig. 3. The mean ratio of the skeletonized pixel areal tubule pixel area for each group was calculated (Fig. 4). Group 3, representing stages VII-VIII, showed a significantly lower value ($p < 0.05$) than all other groups, indicating that these stages contain the least amount of tubulin. Group 5, representing stages XII-XIV and 1-11, contained the greatest amount of tubulin ($p < 0.05$). Groups 1, 2 and 4 were equal in value and contained a moderate level of tubulin. Group 1, representing stages III-V, contained the least amount of α -tubulin, whereas group 4 contained a 67% greater amount of α -tubulin. Groups 2 and 3 were similar in content at a moderate level, but differed significantly from the other groups.

Discussion

This study presents a comprehensive account of stage-specific tyrosinated α -tubulin staining patterns in Sertoli cells of rat seminiferous tubules. These results, using intact seminiferous tubules, confirm a previous study by Vogl (1988) using epithelial fragments, and demonstrate changes in microtubule distribution during spermatogenesis in the rat. The morphological and digital procedures outlined establish a common analytical method that may be used as a standard for future studies of Sertoli cell microtubules. The data show significant differences in α -tubulin content when tubules are grouped according to staining patterns.

This study demonstrates that a commonly used fixative (Bouin's) and routine embedding media (paraffin) are sufficient for immunostaining of α -tubulin in cross-sections of the rat testis. A commercially available antibody was also used, which ensures consistency between reports and provides a common basis for comparison between studies. Previous studies of Sertoli cell microtubules employed various generic tubulin antibodies or antibodies obtained from private laboratories. However, many non-specific α - and β -tubulin antibodies produce homogeneous staining

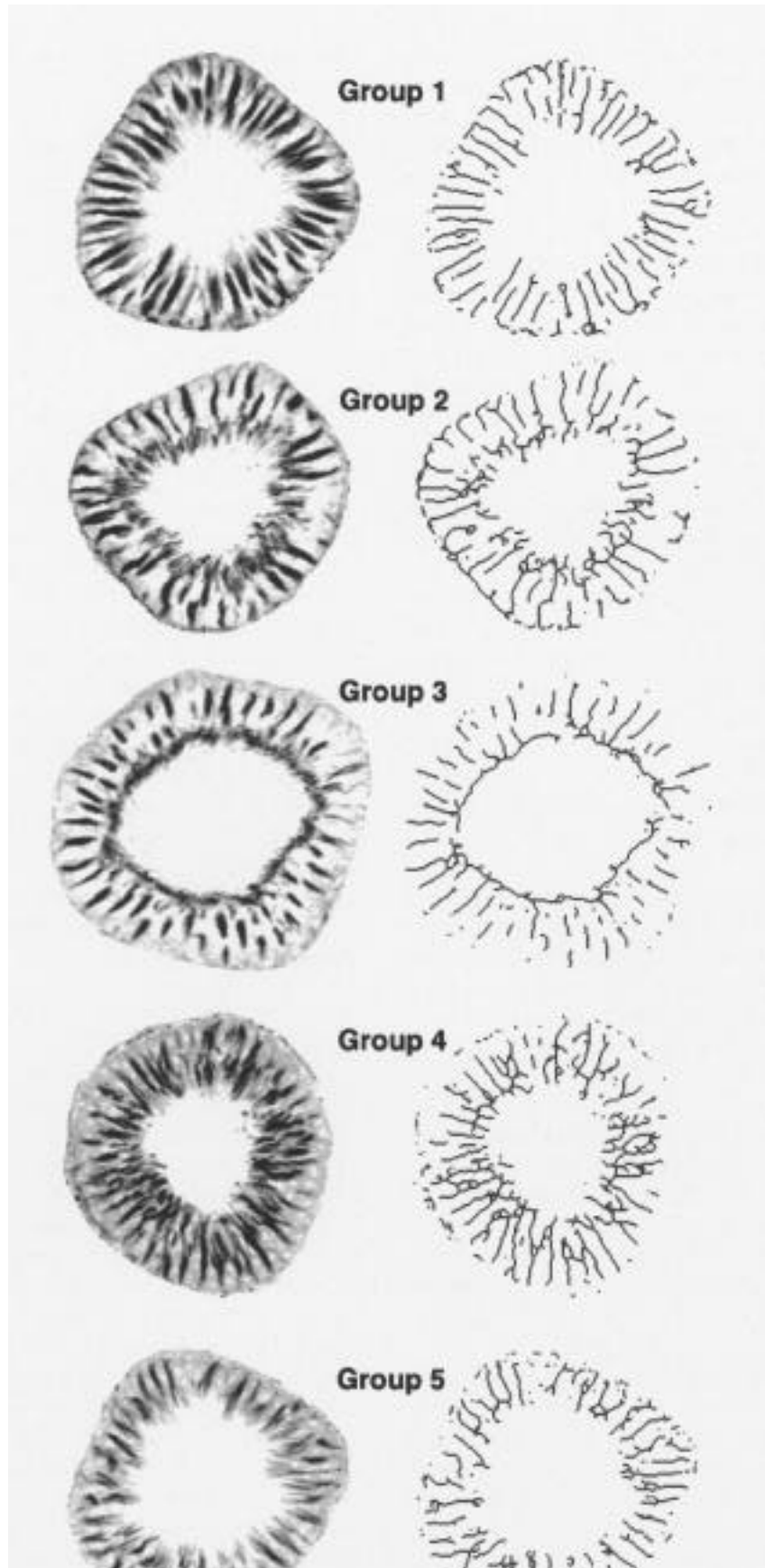


Fig. 3 Representative images of immunostaining for tyrosinated α -tubulin in rat seminiferous tubules grouped by stages having similar staining patterns, with representative skeletonized digital images for each group. Group 1 (Stages III-V) has a pattern of long straight lines that change to mixed long and short lines with luminal branches in group 2 (stages VI-early V 11). Group 3 (stages late VII-VIII) has a nearly continuous line of tubulin encircling the lumen, which becomes highly branched in group 4 (stages IX-XI). Group 5 (stages XII-XIV, I-II) has much less branching in both the basal and luminal regions. x 280.

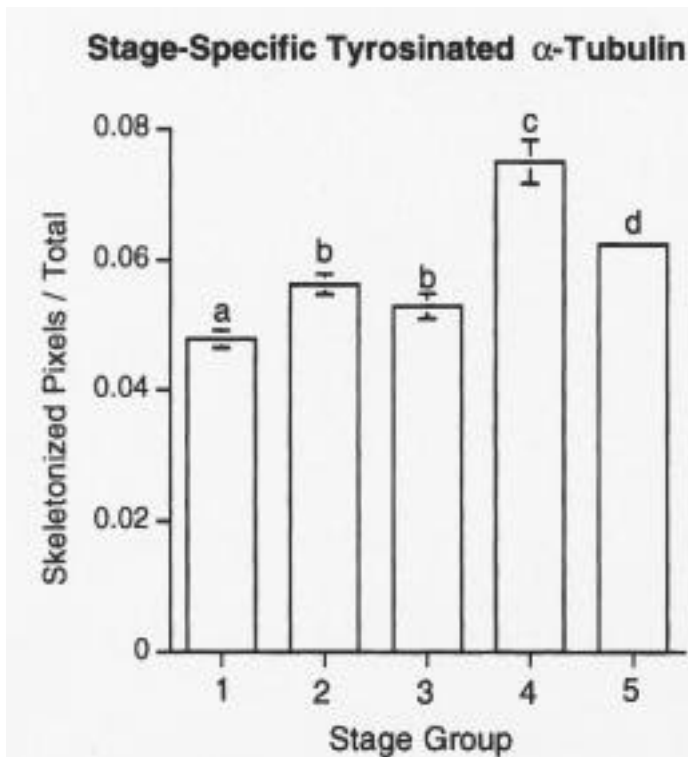


Fig. 4 Stage-specific tyrosinated α -tubulin. Mean \pm SEM ratios of skeletonized tubulin pixels/total number of pixels per tubule are shown by stage groups. Group 1, stages III-V; group 2, stages VI-early VII; group 3, stages late VII-VIII; group 4, stages IX-XI; group 5, stages XII-XIV, 1-11. Columns with different letters are significantly different ($p < 0.05$).

patterns throughout the stages of spermatogenesis, which may explain conflicting reports of stage-specific tubulin staining patterns (Oke & Suarez-Quian, 1993). This study and that of Hermo and co-workers (1991) clearly show that antibody to tyrosinated α -tubulin produces an elaborate staining pattern that changes over the course of spermatogenesis. Tyrosinated tubulin subunits are associated with labile populations of microtubules (Dustin, 1984). The abundance of tyrosinated tubulin-containing microtubules within Sertoli cells suggests a dynamic population that is correlated with the remarkable morphological changes that Sertoli cells undergo as spermatogenesis progresses through stages in the cycle (Parvinen, 1993; Russell, 1993).

Tyrosinated α -tubulin staining patterns are representative of specific distributions of Sertoli cell microtubules within the cytoplasmic body and apical processes. In this study changes in the characteristic distribution of microtubules corresponded to stage-specific changes in the location of elongating spermatids within the epithelium (Figs 1 and 2). Microtubules in stages III-V completely surrounded the elongating spermatid heads that were buried within deep Sertoli cell crypts. This location of the spermatids resulted in a wide 'band-like' tubulin staining pattern. As the elongate spermatids moved toward the lumen, microtubules condensed into long, narrow 'cablelike' patterns present in stages VI-VIII. In stage VIII tubules, prior to spermiation, a linear tubulin staining

pattern was appreciated around the step 8 spermatids (whose nuclei were beginning to elongate). This staining is coincident with the formation of junctions (ectoplasmic specializations) between the Sertoli cell and elongating spermatids (Russell et al., 1988; de Franca et al., 1993). This finding suggests that 'new' microtubules could be forming at the Sertoli cell membrane where it contacts step 8 and 9 spermatids. This hypothesis is supported by Vogl's recent study, which demonstrated that microtubule nucleation occurs at a peripheral site in the Sertoli cell cytoplasm (Vogl et al., 1995). This hypothesis is also consistent with the reverse polarity of Sertoli cell microtubules (Redenbach & Vogl, 1991). Finally, this observation suggests that zones of germ cell-Sertoli cell contact may contain the components responsible for microtubule nucleation, which is also consistent with the proposed role of microtubules in the translocation of elongate spermatids within the seminiferous epithelium (Vogl et al., 1993).

A quantitative procedure was developed using image analysis, to further characterize stage-specific immunoperoxidase staining patterns for tyrosinated α -tubulin. A major limitation of enzyme-linked immunohistochemistry is the fact that enzyme reaction products for visualization of antigens are poorly controlled. Therefore the relationship between reaction product and amount of antigen present is not linear. This limitation was partially addressed by using a consistent section thickness and standardization of immunostaining and image collection procedures. To reduce the amount of variation due to reaction product deposition, digital filters were employed to reduce noise, to smooth and sharpen the image and to reduce the tubulin staining pattern to a single pixel width using the 'Skeletonize' filter.

The skeletonized tubulin staining had a characteristic appearance in each group, which was representative of the whole tubule staining pattern. Long tubulin lines extended from the cellular base to the lumen, representing microtubules in the longitudinal plane of the Sertoli cell. Shorter lines represented an oblique section through the Sertoli cell and areas reduced to 1-2 pixels represented transverse sections. Variation in length of the tubulin skeletons appears to coincide with changes in Sertoli cell morphology at different stages of the cycle. Stages in group I contained the greatest number of long regularly spaced lines of tubulin. This probably represents the fact that the Sertoli cell body diameter is greatest in stages III-V, in which the elongating spermatids are in deep crypts. In groups 2 and 3, representing stages VI-VIII, the Sertoli cell body had its smallest diameter and the body region appeared to be contorted. Thus, the likelihood of an oblique section through the Sertoli cell body was greater, and increasing numbers of shorter strands of tubulin were present in stages VII and VIII.

There was a major change in the staining pattern between groups 2 and 3. Staining near the lumen changed from a wide irregular appearance in group 2 to a thin, compacted

form in Group 3, coincident with the alignment of elongate spermatids near the lumen in preparation for spermiation. This change reduced the skeletonized tubulin from an intricate branching pattern at the luminal edge to a single linear ring. In groups 4 and 5, elaborate branching patterns were seen, coincident with the hypothesized nucleation of microtubules around newly elongating spermatids in stages IX and X (Vogl et al., 1995). In these groups, the branching patterns resulted in narrow base and body regions in the Sertoli cell; however the cytoplasmic processes spread broadly in the luminal one-half to two-thirds of the epithelium, as the Sertoli cell extended its cytoplasm around the elongating spermatids. This extensive branching pattern was responsible for the increase in tubulin seen in the groups following spermiation.

These data provide a foundation for evaluating α -tubulin staining patterns in testicular cross-sections. Familiarity with the characteristic staining patterns, which show significant differences in the various stages of the cycle of the seminiferous epithelium, will greatly aid the recognition of alterations in microtubule-dependent processes in the Sertoli cell.

Appendix. Skeletonized area of tubulin immunostaining patterns

This macro procedure was written written by John R. Wenz in the NIH Image Pascal-like macro programming language (1/12/95, revised 6/96).

macro 'Tubulin Skeleton [this macro performs filtering Area [S]';
 procedures, segments tubulin staining by thresholding, makes the image binary, skeletonizes the image, measures skeleton pixel area, then measures whole tubule area, calculates proportion of tubulin skeleton pixel area/total tubule pixel area and reports these values for all slices of a stack in table form.]

```
var
  sum, total, i,j,n, s,t: integer; count I count2:
real; begin;
  CheckForStack;
  SetUser I Label('Tubulin Area');
  SetUser2label('Tub/Tot');
  LabelParticles(false);
  OutlineParticles(false);
  ResetCounter; for s:= I to 10
    do begin; SelectSlice(s);
      SetCounter(IO);
      SelectAll;
      Duplicate('Temp');
      Smooth; ReduceNoise;
```

```
Sharpen;
Autothreshold;
MakeBinary;
Skeletonize;
Measure;
Dispose;
sum:=0;
for i:=1 I to rCount do sum:=histogram[255];
rUser I [s]: =sum;
SetParticleSize(1,999999);
SetDensitySlice(1,255);
SetCounter(IO);
AnalyzeParticles;
Undo;
sum:=0;
for i:= I I to rCount do sum:=sum+rArea[i];
rArea[s]:=sum;
SetDensitySlice(0,0);
for i:=1 I to rCount do rUser2[s]:=rUser1 [s]/rArea[s];
UpdateResults;
end;
SetCounter(IO);
ShowResults;
CopyResults;
end;
```

ACKNOWLEDGEMENTS

We thank Dr Martha Zimmerman and Eman Jassim for outstanding technical assistance. We are also grateful to Dr Masaaki Nakai for his helpful discussions and suggestions during this study. This project was supported in part by NIH grant PHS-RO I ES07832.

REFERENCES

- Allard, E.K., Johnson, K.J. and Boekelheide, K. 1993. Colchicine disrupts the cytoskeleton of rat testis seminiferous epithelium in a stage-dependent manner. *Biol. Reprod.*, 48, 143-153.
- Amlani, S. and Vogl, A.W. 1988. Changes in the distribution of microtubules and intermediate filaments in mammalian Sertoli cells during spermatogenesis. *Anat. Rec.*, 220, 143-160.
- Creasy, D.M. 1997. Evaluation of testicular toxicity in safety evaluation studies - the appropriate use of spermatogenic staging [review]. *Toxicol. Pathol.*, 25, 119-131.
- de Franca, L.R., Ghosh, S., Ye, S.J. and Russell, L.D. 1993. Surface and surface-to-volume relationships of the Sertoli cell during the cycle of the seminiferous epithelium in the rat. *Biol. Reprod.*, 49, 1215-1228.
- Dustin, P. 1984. *Microtubules*. 2nd edn. Springer-Verlag. New York, 462.
- Hermo, L., Oko, R. and Hecht, N.B. 1991. Differential post-translational modifications of microtubules in cells of the seminiferous epithelium of the rat: a light and electron microscope immunocytochemical study. *Anat. Rec.* 229, 31-50.
- Hess, R.A. 1990. Quantitative and qualitative characteristics of the stages and transitions in the cycle of the rat seminiferous epithelium: light microscopic observations of perfusion-fixed and plastic-embedded testes. *Biol. Reprod.*, 43, 525-542.
- Ireland, C.M., Gull, K., Gutteridge, W.E. and Pogson, C.I. 1979. The interaction of benzimidazole carbamates with mammalian microtubule protein. *Biochem. Pharmacol.*, 28, 2680-2682.
- Leblond, C.P. and Clermont, Y. 1952. Definition of the stages of the cycle of the seminiferous epithelium in the rat. *Ann. N.Y. Acad. Sci.*, 55, 548-573.

- Nakai, M. and Hess, R.A. 1994. Morphological changes in the rat Sertoli cell induced by the microtubule poison carbendazim. *Tissue Cell*, 26, 917-927.
- Oke, B. and Suarez-Quian, C. 1993. Localization of secretory, membrane-associated and cytoskeletal proteins in rat testis using an improved immunocytochemical protocol that employs polyester wax. *Biol. Reprod.*, 48, 621-631.
- Parvinen, M. 1993. Cyclic function of Sertoli cells. In: *The Sertoli cell* (eds L.D. Russell and M. D. Griswold), Cache River Press, Clearwater, FL, 39-86.
- Redenbach, D.M. and Vogl, A.W. 1991.** Microtubule polarity in Sertoli cells: a model for microtubule-based spermatid transport. *Eur. J. Cell Biol.*, 54, 277-290.
- Redenbach, D.M., Boekelheide, K. and Vogl, A.W. 1992. Binding between mammalian spermatid-ectoplasmic specialization complexes and microtubules. *Fur. J. Cell Biol.*, 59, 433-448.
- Richburg, J.H., Redenbach, D.M. and Boekelheide, K. 1994. Seminiferous tubule fluid secretion is a Sertoli cell microtubule-dependent process inhibited by 2,5-hexanedione exposure. *Toxicol. Appl. Pharmacol.*, 128, 302-309.
- Russell, L.D. 1993. Form, dimensions, and cytology of mammalian Sertoli cells. In: *The Sertoli cell* (eds L.D. Russell and M.D. Griswold), Cache River Press, Clearwater, FL, 1-37.
- Russell, L.D., Malone, J.P. and MacCurdy, D.S. 1981. Effect of the microtubule disrupting agents, colchicine and vinblastine, on seminiferous tubule structure in the rat. *Tissue Cell*, 13, 349-367.
- Russell, L.D., Goh, J.C., Rashed, R.M. and Vogl, A.W. 1988. The consequences of actin disruption at Sertoli ectoplasmic specialization sites facing spermatids after in vivo exposure of rat testis to cytochalasin D. *Biol. Reprod.*, 39, 105-118.
- Russell, L.D., Ettl, R.A., Sinha Hikim, A.P. and Clegg, E.D. 1990. Histological and histopathological evaluation of the testis. Cache River Press, Clearwater, FL, 286.
- Vogl, A.W. 1988. Changes in the distribution of microtubules in rat Sertoli cells during spermatogenesis. *Anat. Rec.*, 222, 34-41.
- Vogl, A.W., Linck, R.W. and Dym, M. 1983. Colchicine-induced changes in the cytoskeleton of the golden-mantled ground squirrel (*Spermophilus lateralis*) Sertoli cells. *Am. J. Anat.*, 168, 99-108.
- Vogl, A.W., Pfeiffer, D.C., Redenbach, D.M. and Grove, B.D. 1993. Sertoli cell cytoskeleton. In: *The Sertoli cell* (eds L.D. Russell and M.D. Griswold), Cache River Press, Clearwater, FL, 39-86.
- Vogl, A.W., Weis, M. and Pfeiffer, D.C. 1995. The perinuclear centriole-containing centrosome is not the major microtubule organizing center in Sertoli cells. *Eur. J. Cell Biol.*, 66, 165-179.